K. O. Martin, and H. A. Levy), ORFFE (locally modified, calculations of distances, angles, and least-squares planes with standard deviations by Busing, Martin, and Levy), and ORTEP (thermal ellipsoid drawing program, by C. K. Johnson).
(14) P. W. R. Corfield, R. J. Doedens, and J. A. Ibers, *Inorg. Chem.*, **6**, 197 (1967).
(15) W. C. Hamilton, *Acta Crystallogr.*, **18**, 502 (1965).
(16) M. R. Churchill, *Inorg. Chem.*, **12**, 1213 (1973).
(17) Supplementary material.
(18) W. O. Gillum, J. C. Huffman, W. E. Streib, and R. A. D. Wentworth, *Chem. Commun.*, 843 (1969).
(19) M. R. Churchill and A. H. Reis, *Inorg. Chem.*, **11**, 1811 (1972); **12**, 2280 (1973); *J. Chem. Soc., Dalton Trans.*, 1570 (1973).
(20) D. L. Kepert, *Inorg. Chem.*, **11**, 1561 (1972); *Prog. Inorg. Chem.*, **23**, 1 (1977).
(21) A. Avdeef and J. P. Fackler, Jr., *Inorg. Chem.*, **14**, 2002 (1975).
(22) B. A. Cartwright, D. M. L. Goodgame, I. Jeeves, P. O. Langguth, Jr., and A. C. Skapski, *Inorg. Chim. Acta*, **24**, L45 (1977).
(23) R. Eisenberg and H. B. Gray, *Inorg. Chem.*, **6**, 1844 (1967).
(24) F. A. Cotton and G. Wilkinson in "Advanced Inorganic Chemistry", 3rd ed, Interscience, New York, N.Y., 1972, p 120.
(25) J. R. Dilworth in "Proceedings of the Climax First International Conference on the Chemistry and Uses of Molybdenum", P. C. H. Mitchell, Ed., Climax Molybdenum Co., London, 1973, p 269.
(26) M. Cowie and M. J. Bennett, *Inorg. Chem.*, **15**, 1584 (1976).
(27) B. Spivack and Z. Dori, *Coord. Chem. Rev.*, **17**, 99 (1975).
(28) J. I. Gelder, J. H. Enemark, G. Wolterman, D. A. Boston, and G. P. Haight, *J. Am. Chem. Soc.*, **97**, 1616 (1975).
(29) M. W. Bishop, J. Chatt, J. R. Dilworth, M. B. Hursthouse, and M. Motevalli in "Proceedings of the Climax Second International Conference on the Chemistry and Uses of Molybdenum", P. C. H. Mitchell and A. Seaman, Ed., Climax Molybdenum Co., London, 1976, p 252.
(30) G. F. Brown and E. I. Stiefel, *Inorg. Chem.*, **12**, 2140 (1973); W. P. Bosman and A. Nieupoort, *ibid.*, **15**, 775 (1976).
(31) P. M. Boorman, C. D. Garner, F. E. Mabbs, and T. J. King, *J. Chem. Soc., Chem. Commun.*, 663 (1974).
(32) G. Bunzey and J. H. Enemark, *Inorg. Chem.*, **17**, 682 (1978).
(33) K. Yamanouchi and J. H. Enemark, to be submitted for publication; tox is 8-mercaptoquinolinate.
(34) W. R. Scheidt, *Inorg. Chem.*, **12**, 1758 (1973).
(35) R. W. G. Wyckoff in "Crystal Structures", Vol. 6, Part 1, 2nd ed, Wiley, New York, N.Y., 1971, p 1, 272–278.
(36) J. L. Martin and J. Takats, *Inorg. Chem.*, **14**, 1358 (1975).
(37) M. Cowie and M. J. Bennett, *Inorg. Chem.*, **15**, 1589 (1976).
(38) M. Cowie and M. J. Bennett, *Inorg. Chem.*, **15**, 1595 (1976).
(39) A. E. Smith, G. N. Schrauzer, V. P. Mayweg, and W. Heinrich, *J. Am. Chem. Soc.*, **87**, 5798 (1965).
(40) C. G. Pierpont and R. Eisenberg, *J. Chem. Soc. A*, 2285 (1971).
(41) K. N. Raymond, S. S. Isied, L. D. Brown, F. R. Fronczek, and J. H. Nibert, *J. Am. Chem. Soc.*, **98**, 1767 (1976).
(42) E. I. Stiefel, R. Eisenberg, R. C. Rosenberg, and H. B. Gray, *J. Am. Chem. Soc.*, **88**, 2956 (1966).
(43) R. Hoffmann, J. M. Howell, and A. R. Rossi, *J. Am. Chem. Soc.*, **98**, 2484 (1976).
(44) E. I. Stiefel, W. E. Newton, and N. Pariyadath in "Proceedings of the Climax Second International Conference on the Chemistry and Uses of Molybdenum", P. C. H. Mitchell and A. Seaman, Ed., Climax Molybdenum Co., London, 1976, p 265.
(45) E. I. Stiefel and J. K. Gardner in "Proceedings of the Climax First International Conference on Chemistry and Uses of Molybdenum", P. C. H. Mitchell, Ed., Climax Molybdenum Co., London, 1973, p 272.
(46) I. N. Duglav and Z. I. Usmanov, *Zh. Strukt. Khim.*, **16**, 312 (1975).

Contribution from the ARC Unit of Nitrogen Fixation, University of Sussex,
Brighton, BNI 9QJ, United Kingdom, the Empire State Plaza Laboratories,
New York State Department of Health, Albany, New York 12208, and the Department of Chemistry,
The State University of New York at Albany, Albany, New York 12222

Synthesis, Structure, and Properties of Asymmetric Benzoyldiazenido and Thiobenzoyldiazenido Complexes of Molybdenum

MICHAEL W. BISHOP,[1a] JOSEPH CHATT,[1a] J. R. DILWORTH,[1a] J. R. HYDE,[1b] S. KIM,[1c]
K. VENKATASUBRAMANIAN,[1b] and JON ZUBIETA*[1b]

Received March 3, 1978

The synthesis of the compounds of general formula $[Mo_2O(S_2CNR)_2(YC_6H_4CXN_2)_2]\cdot Sol$, X = S and O, Y = H and Cl, and Sol = CH_2Cl_2 and $CHCl_3$, is reported. The compounds were characterized by elemental analyses and infrared, electronic, and ^1H NMR spectroscopy. The ^1H NMR spectra exhibited a number of alkyl resonances, suggesting that the dithiocarbamate ligands are nonequivalent. The molecular structures of the compounds $[Mo_2O(S_2CNEt_2)_2(C_6H_5CON_2)_2]\cdot CH_2Cl_2$ and $[Mo_2O(S_2CNEt_2)_2(ClC_6H_4CSN_2)_2]\cdot CHCl_3$ were revealed in single-crystal X-ray diffraction studies. The structures are analogous and shown to be asymmetric dinuclear complexes with bridging benzoyldiazendio or thiobenzoyldiazenido ligands. The nonplanar Mo_2N_2 rhombus is common to both structures and exhibits a nearly identical geometry in the two derivatives. The geometries about the square-pyramidal Mo2 sites are also constant. The Mo1 sites are approximately trigonal prismatic, the coordination polyhedra constrained by the geometric requirements of sulfur vs. oxygen coordination. Voltammetric studies of the dimers indicate a reversible one-electron reduction, followed by an irreversible cathodic process at more negative potentials. The redox behavior of the dimers is discussed and contrasted with that of the symmetrical dimers $Mo_2O_3(S_2CX)_4$, X = $-NR_2$, $-OR$, and $-SR$.

Introduction

The coordination chemistry of molybdenum in its higher oxidation states (IV to VI) has received a great deal of attention, particularly because of the possible relationship of these species to the redox-active molybdoenzymes[2,57] and the general interest in polynuclear metal compounds.[3,59] In particular, the iron–molybdenum protein component of nitrogenase from *Azotobacter vinelandii*,[4] *Clostridium pasteurianum*,[5] and *Klebsiella pneumoniae*[6] and xanthine oxidase[7] all contain two molybdenum atoms per mole of enzyme. The proposal has been made that the two molybdenum atoms are at the active site and function in a concerted fashion during catalysis.[8] Although a number of oxidation states have been postulated for the molybdenum atoms in the native proteins,[7b] there is no direct evidence for the oxidation state in the nitrogenase systems.

The importance of molybdenum in these redox-active proteins and the speculation that dimeric species involving sulfur coordination may be relevant to the active-site geometry[2,7b] have prompted a number of studies on the chemical,[8–10] electrochemical,[11] and structural aspects[12–23] of dimeric molybdenum complexes with sulfur-containing ligands.

The structural chemistry of dimeric molybdenum complexes in the higher oxidation states is dominated by oxo- or sulfido-bridged groupings (**1a**–**2e**). A number of complexes with the μ-oxo geometry **1a**[14] or **1b**[12,13,15,24] have been structurally

0020-1669/78/1317-2917$01.00/0

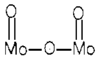

1a

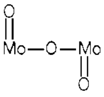

1b

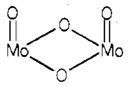

1c

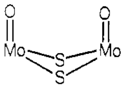

2a

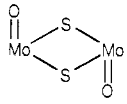

2b

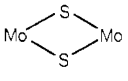

2c

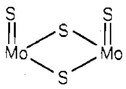

2d

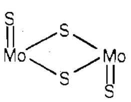

2e

characterized. There are numerous examples of the *cis*-di-μ-oxo coordination type, **1c**;[16,17,25,26] the existence of stable di-μ-sulfido-bis(oxomolybdenum) complexes is well documented,[3a,20,21,23,27,28] and two distinct geometries syn-bent, **2a**, and anti-planar, **2b**, have been established.[23] Although fewer examples are available, exclusive sulfido coordination has been observed for $[MoS(SCNR_2)(S_2CNR_2)]_2$,[22] $[Mo_2S_4(S_2CNR_2)_2]$,[19] and $[Mo_2S_4(S_2C_2H_4)_2]^{2-}$.[60] A common feature of the dimeric complexes is nearly identical coordination geometry about the molybdenum atoms of the dimer unit. The electrochemical behavior of the dimers tends to be complex and dominated by irreversible processes.[11,15]

As part of our general studies of the chemistry of higher oxidation state complexes of molybdenum and in particular their reactions with substituted hydrazines,[29a] we have investigated the interactions of the dioxo complexes $[MoO_2(S_2CNR_2)_2]$ (R_2 = Me_2, Et_2, $((CH_2)_5)_2$) with benzoyl- and thiobenzoylhydrazines. In the presence of excess dithiocarbamate, benzoylhydrazine reacts in refluxing methanol to give the benzoyldiazenido complexes $[Mo(N_2COPh)(S_2CNR_2)_3]$ containing a linear Mo–N–N linkage.[29b] Thioaroylhydrazines generally undergo quite different reactions from aroylhydrazines, as with acidified molybdate where the former give complexes of the type $[Mo(HNNCSAr)_3]$ (Ar = phenyl or substituted phenyl),[29a] whereas aroylhydrazines form no isolable complexes under similar conditions.

In this paper, we describe the full details of the synthesis, electrochemical investigation, structural studies, and spectroscopic properties of a number of unusual dimeric complexes formed from molybdenum dioxobis(dithiocarbamato) complexes and the hydrazines $PhCXNHNH_2$ (X = O, S).[29c]

Experimental Section

The reactions were carried out under nitrogen using dried degassed solvents, but the recrystallizations were performed with reagent grade solvents in air. Molecular weights were determined using a Hitachi Perkin-Elmer Model 115 osmometer and infrared spectra were recorded as Nujol mulls using a "Pye Unicam" SP 2000 spectrometer. ^1H NMR spectra were measured in dideuteriodichloromethane at 100 MHz using a Jeol P.S. 100 spectrometer with tetramethylsilane as internal standard. Microanalyses were carried out by Mr. and Mrs. Olney at the University of Sussex and by A. G. Bernhardt Microanalytical Laboratories, West Germany.

The complexes $[MoO_2(S_2CNR_2)]$ (R_2 = Me_2, Et_2, $((CH_2)_5)_2$) were prepared by the literature method[51] as were benzoylhydrazine[53] and the thioaroylhydrazines.[52]

Bis(benzoyldiazenido)bis(diethyldithiocarbamato)oxodimolybdenum (3). Dioxobis(diethyldithiocarbamato)molybdenum(VI) (0.5 g), benzoylhydrazine hydrochloride (0.25 g), and triphenylphosphine (0.3 g) in methanol (30 mL) were heated under reflux for 0.25 h. After the mixture was allowed to stand overnight, the *complex* precipitated from solution and was recrystallized as red needles from dichloromethane–methanol. The dichloromethane of crystallization was removed by pumping at 60 °C and 10^{-2} mmHg giving a red powder.

Bis(thiobenzoyldiazenido)bis(dimethyldithiocarbamato)oxodimolybdenum (4a). Dioxobis(dimethyldithiocarbamato)molybdenum(VI) (0.5 g) and thiobenzoylhydrazine (0.3 g) in methanol (40 mL) were heated under reflux for 0.3 h. On cooling of the solution, the complex was deposited as a very dark precipitate and was recrystallized from dichloroethane–methanol as tiny red needles (0.24 g, 48%).

Complexes **4b**, **4c**, **4d**, **4e**, and **4** were prepared similarly to complex **4a**, using appropriate dioxodithiocarbamato complex and thioaroylhydrazine in yields of 45–66%.

Crystal Preparation. The benzoyldiazenido derivative, $Mo_2O(S_2CNEt_2)_2(C_6H_5CON_2)_2 \cdot CH_2Cl_2$ (**3**), was crystallized from dichloromethane/methanol by slow evaporation at 10 °C. The ^1H NMR spectrum of the recrystallized material exhibited a proton resonance consistent with a dichloromethane molecule of crystallization, and this was later confirmed by the density of the crystals and the solution of the structure.

The thiobenzoyldiazenido derivative $Mo_2O(S_2CNEt_2)_2(ClC_6H_4CSN_2)_2 \cdot CHCl_3$ (**4**) was crystallized from chloroform/methanol by slow evaporation. Attempts to recrystallize from carbon disulfide, tetrahydrofuran, and benzene were unsuccessful, generally yielding oils or amorphous solids. The ^1H NMR spectrum of the crystallized complex again displayed a resonance attributable to a molecule of solvation. The presence of chloroform in the lattice was confirmed by the solution of the structure.

Collection and Reduction of Diffraction Data. Preliminary cell dimensions were obtained from Weissenberg and precession photographs of the crystals taken with Cu Kα radiation (λ 1.5418 Å). Using the approximate cell dimensions obtained by film measurement, 20 reflections with $16 < 2\theta < 23°$ were accurately centered in the counter window of a Picker full-circle automated diffractometer (Mo Kα radiation). A least-squares procedure was used to obtain a best fit between the observed and calculated values of χ, ϕ, and 2θ for these reflections. The cell parameters and relevant crystal data are presented in Table I.

Intensity data were collected on the Picker diffractometer using Mo Kα (λ 0.7107 Å) radiation filtered through zirconium foil. A scan speed of 1°/min was employed in measuring each reflection by the moving crystal–moving counter technique with a scan range in 2θ of 2°, plus an allowance for the splitting of the Kα_1 and Kα_2 radiation. The background for each reflection was determined by 10 s stationary counts at each end of the scan range. The net count (N) was calculated as $N = T - (BG1 + BG2) \cdot SCT/20$, where T is the total integrated peak intensity, BG1 and BG2 are the background counts, and SCT is the total measuring time for the peak in seconds. Four standard reflections were employed to monitor diffractometer and crystal stability. The fluctuation in the integrated intensities of the standards was no greater than that expected from Poisson statistics, totaling 1.5% over the period of the data collection.

The observed intensities were corrected for background, Lorentz, and polarization effects. Only reflections with $I > 2.5\sigma(I)$ were included in the refinement.

Solution and Refinement of the Structures. In both cases the initial Patterson map revealed the positions of the two molybdenum and four sulfur atoms.

Full-matrix least-squares refinement was based on F, and the function was minimized as $\sum w(|F_o| - |F_c|)^2$. The weights w were taken as $(2F_o/\sigma(F_c^2))^2$ where $|F_o|$ and $|F_c|$ are the observed and calculated structure factor amplitudes. Atomic scattering factors for nonhydrogen atoms were taken from Cromer and Waber.[30] Scattering factors for hydrogen were those of Stewart, Davidson, and Simpson.[31] The anomalous dispersion corrections for molybdenum, sulfur, and chlorine were included. The programs used in the refinement were those compiled in the 1972 version of the X-ray system of Stewart et al.[32] and operated on the Univac 1110 computer. Difference Fourier syntheses phased on the six heavy atoms revealed the remaining part of the structures. Refinement of positional parameters and individual isotropic temperature factors for the atoms contained in the dimeric units converged at values of 0.174 and 0.184 for **3** and **4**, respectively, for the conventional R factor. At this stage the difference Fourier maps revealed the presence of the solvent molecules. The $CHCl_3$ molecule found in structure **4** presented no difficulties. These atomic positions and anisotropic temperature factors for all noncarbon and nonhydrogen atoms were introduced. Five cycles of full-matrix least-squares refinement converged to $R = 0.076$ and $R_w = 0.086$ where $R = \sum||F_o| - |F_c||/\sum|F_o|$ and $R_w = (\sum w(|F_o| - |F_c|)^2/\sum w|F_o|^2)^{1/2}$.

Table I. Experimental Summary of Crystal Data

	$[Mo_2O(S_2CNEt_2)_2(C_6H_5CON_2)_2]\cdot CH_2Cl_2$	$[Mo_2O(S_2CNEt_2)_2(ClC_6H_4CSN_2)_2]\cdot CHCl_3$
formula wt	855.49	991.03
a, Å	17.526 (8)	17.362 (8)
b, Å	10.800 (9)	11.888 (9)
c, Å	9.536 (9)	20.177 (8)
α, deg	107.95 (2)	90.00
β, deg	92.88 (1)	113.88 (2)
γ, deg	85.07 (1)	90.00
volume, $Å^3$	1728.00	3796.70
cryst form	triclinic	monoclinic
systematic absences	none	$0k0$, $k = 2n + 1$; $h0l$, $h = 2n + 1$
space group	$P\bar{1}$	$P2_1/a$
Z	2	4
ρ(calcd), g cm^{-3}	1.64	1.73
ρ(found), g cm^{-3}	1.65 (2)	1.75 (2)
$F(000)$	860.00	1976.00
λ(Mo)	K$\bar{\alpha}$, 0.7107 Å	K$\bar{\alpha}$, 0.7107 Å
cryst dimens	0.17 × 0.35 × 0.16 mm	0.13 × 0.31 × 0.12 mm
μ(Mo Kα)	11.32 cm^{-1}; transmission factors varied between 0.792 and 0.861	13.43 cm^{-1}; transmission factors varied between 0.789 and 0.869
reflect	2246 symmetry-independent reflections for $2 < 2\theta \leqslant 40°$ with $I_0 > 2.5\sigma(I_0)$ (3220 collected)	2458 symmetry-independent reflections for $2 < 2\theta \leqslant 40°$ with $I_0 > 2.5\sigma(I_0)$ (3111 collected)

The error in an observation of unit weight, $[\sum w\Delta^2/(NO - NV)]^{1/2}$, was 1.89.

In the case of compound **3**, the chlorine atoms of the CH_2Cl_2 group were clearly evidenced on the Fourier map, although some positional disorder was indicated. The peak assigned to the carbon atom was 2.0 e Å^{-3} and suggested considerable disorder. Since the major purpose of this work was the determination of the molecular structures of the dimers and since the analogous thiobenzoyldiazenido complex was free of disorder, the problem was not pursued further.[33] The solvent molecule positional parameters and anisotropic temperature factors for molybdenum, sulfur, oxygen, and chlorine atoms were included in the refinement which converged to $R = 0.069$ and $R_w = 0.080$. The error in an observation of unit weight was 2.13.

Final difference Fourier synthesis on both structures revealed no excursions in electron density greater than 0.7 e Å^{-3}, on a scale where the average value for a carbon atom is 6 eÅ^{-3}. Maximum excursions of electron density occurred at 0.5 Å from the Mo positions and at positions consistent with hydrogen locations. Tables of the observed and calculated structure factors are available.

Electrochemical Studies. Electrochemical measurements were performed in $CH_2Cl_2|0.1$ M $[n\text{-}Bu_4N]PF_6$ or acetone$|0.1$ M $[n\text{-}Bu_4N]PF_6$ vs. Ag|AgCl|0.1 M LiCl reference electrode or an isolated saturated calomel electrode. All potentials are reported with respect to the SCE. A three-electrode, iR-compensated system with a platinum auxiliary electrode was used throughout. Normal pulse voltammetry and cyclic voltammetry were performed at a platinum wire electrode. Cyclic voltammograms were also recorded at vitreous carbon and hanging mercury drop electrodes. The PAR Model 170 electroanalytical system was employed in all measurements. Phase-sensitive ac voltammograms were made at a scan rate of 10 mV/s at 80 Hz with phase angle of 90° with respect to the input alternating potential and with an ac perturbation of 5 mV peak–peak. Normal pulse polarograms were obtained at a scan rate of 10 mV s^{-1} with a pulse frequency of 2.0 pulse s^{-1}. All solvents were degassed with Ar, and all runs were performed under an inert atmosphere at 21 °C. Controlled-potential electrolyses were performed at a platinum mesh or a rotating platinum electrode at a potential +0.25 V beyond the $E_{1/2}$ of the process under investigation.

Results and Discussion

Preparation and Properties of Complexes. In the absence of excess dithiocarbamate, benzoylhydrazine hydrochloride reacts with $[MoO_2(S_2CNEt_2)_2]$ and triphenylphosphine in refluxing methanol to give a red complex of stoichiometry $[Mo_2O(S_2CNEt_2)_2(NNCOPh)_2]$ (**3**). A small amount of the orange benzoyldiazenido complex $[Mo(NNCOPh)(S_2CNEt_2)_3]$ is sometimes also formed but can be readily separated by recrystallization. However, even in the presence of excess dithiocarbamate the only complexes that can be isolated by the reactions of $[MoO_2(S_2CNR_2)_2]$ with the thiobenzoylhydrazines $ArCSNHNH_2$ (Ar = C_6H_5, p-$MeOC_6H_4$, p-ClC_6H_4) are analogues of complex **3**, $[Mo_2O(S_2CNR_2)_2(NNCSAr)_2]$. There was no evidence for the formation of the thiobenzoyldiazenido complexes $[Mo(NNCSPh)(S_2CNR_2)_3]$. The complexes prepared in this manner are summarized in Table II, together with physical and spectroscopic properties.

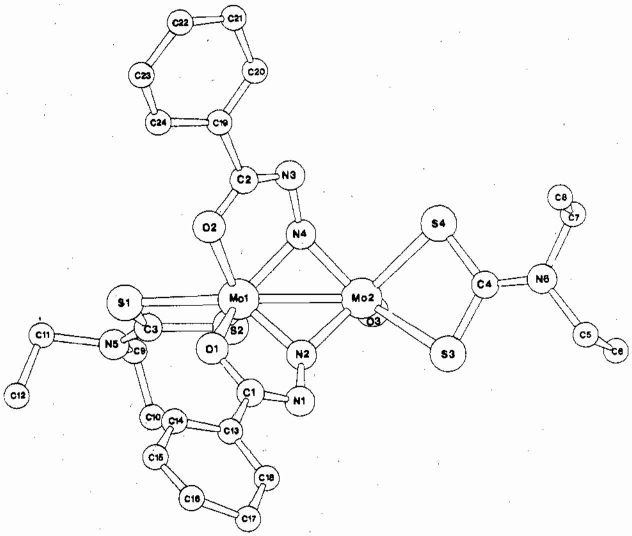

Figure 1. Perspective view of the molecule $Mo_2O(S_2CNEt_2)_2(PhCON_2)_2$ (**3**) showing the atom labeling scheme.

The complexes are all red or pinkish red diamagnetic, crystalline, air-stable solids. Their solutions in 1,2-dichloroethane are nonconducting, and molecular weight measurements, where solubility permitted, indicated that they are dimeric.

Structural Determination. Final positional and thermal parameters for complexes **3** and **4** are given in Tables III and IV. Tables V and VI contain the bond lengths and angles for $[Mo_2O(S_2CNEt_2)_2(C_6H_5CON_2)_2]\cdot CH_2Cl_2$ and Tables VII and VIII the bond parameters for $[Mo_2O(S_2CNEt_2)_2(ClC_6H_4CSN_2)_2]\cdot CHCl_3$. The digits in parentheses in the tables are the estimated standard deviations in the least significant figures quoted. Figures 1 and 2 are perspective views of the molecules giving the atom labeling schemes, while Figures 3 and 4 show the molecular packing in the unit cells. Table IX gives the coefficients of the least-squares planes for the dimers.

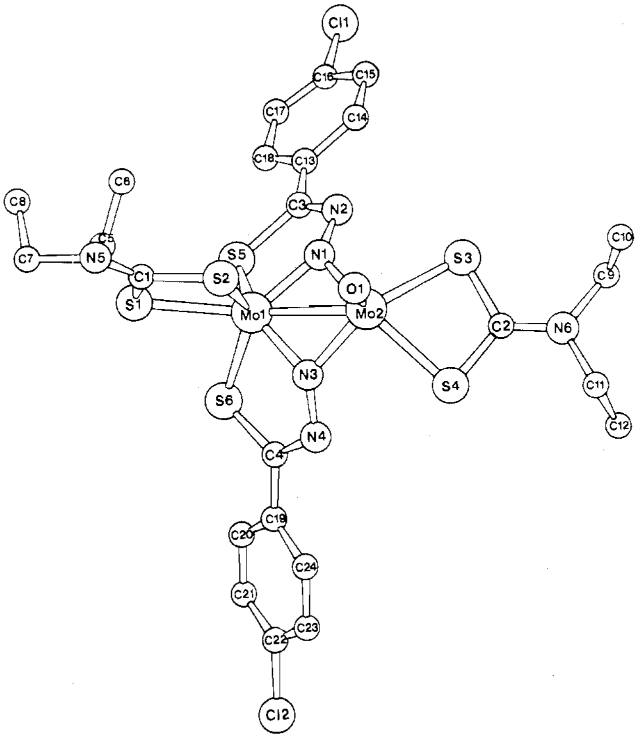

Figure 2. Perspective view of the molecule $Mo_2O(S_2CNEt_2)_2(ClC_6H_4CSN_2)_2$ (**4**) showing the atom labeling scheme.

Both complexes, $[Mo_2(S_2CNEt_2)_2(C_6H_5CON_2)_2]\cdot CH_2Cl_2$ (**3**) and $[Mo_2(S_2CNEt_2)_2(ClC_6H_4CSN_2)_2]\cdot CHCl_3$ (**4**), consist of discrete dimeric molecules. Figures 1 and 2 demonstrate the low overall symmetry of the complexes and the nature of the distinct environments about the molybdenum atoms. The coordination polyhedron about Mo2 in both **3** and **4** is essentially square pyramidal with the Mo atoms displaced toward the apical oxygens, 0.72 Å from the mean plane generated by S3–S4–N2–N4 in **3** and 0.69 Å from the plane S3–S4–N1–N3 in **4** (Table IX). The geometry of the five-coordinated Mo may be compared to that observed in $[Mo_2O_4(S_2CNEt_2)_2]$,[18] $[MoO(S_2CNPr_2)_2]$,[12] $MoO(S_2CS\text{-}i\text{-}Pr)_2$,[38] and $[(C_4H_9)_4N]_2[Mo_2O_2S_2\{S_2C_2(CN)_2\}_2]$,[23] which also exhibit similar square-pyramidal geometry (Table X).

The coordination geometry at the second Mo site is approximately trigonal prismatic, although the variation in donor atoms results in considerable distortion of the coordination polyhedron, as illustrated in Figure 5. In compound **3**, the triangular faces S1–O1–O2 and S2–N2–N4 are not perfectly parallel; displaying a dihedral angle of 170.5°. The angle of twist between the triangular faces is 10.8°. The deviations from regular geometry are not so pronounced in compound **4** where the triangular faces S2–N1–N3 and S1–S5–S6 make a dihedral angle of 177.0° and the angle of twist between the triangular faces is 4.3°. A detailed analysis of the geometry, as suggested by Muetterties and Guggenberger,[50] is presented in Table XI; both the dihedral angle and twist angle criteria are consistent with the distorted trigonal-prismatic description of the coordination polyhedron. The geometry of the polyhedron may be compared to that displayed by $[Mo(S_2C_6H_4)_3]$[34] and $[Mo(S_2C_2H_2)_3]$,[35] where the Mo is formally in the +VI oxidation state and regular trigonal-prismatic coordination is observed, and $[Mo(S_2C_2(CN)_2)_3]^{2-}$, where the Mo oxidation state is formally +IV resulting in a geometry intermediate between octahedral and trigonal prismatic with a dihedral angle of 178° and an angle of twist of 27°. The common features of these trigonal-prismatic and derived structures are metal centers with few d electrons (d^0–d^2) and the presence of a highly delocalized ligand orbital system such

Table II. Complexes of the Type $[Mo_2O(S_2CNR_2)_2(N_2CXAR)_2]$

no.	complex	color	mp[a]	analysis,[b] % C	H	N	S	mol wt[b,c]	^1H NMR,[f] ppm: aryl protons	dithiocarbamato alkyl protons
3	$[Mo_2O(S_2CNEt_2)_2(N_2COPh)_2]$[d]	red	283–286	35.3 (35.1)	3.7 (3.0)	9.8 (9.8)				
4a	$[Mo_2O(S_2CNMe_2)_2(N_2CSPh)_2]$[e]	red	310–313	31.5 (32.2)	2.9 (3.0)	11.0 (11.2)				
4b	$[Mo_2O(S_2CNMe_2)_2(N_2CSC_6N_4\text{-}p\text{-}OMe)_2]$	red	273–278	32.2 (32.7)	3.9 (3.2)	9.8 (10.4)			6.7 m (4) 7.8 m (4)	3.3 m (12)
4c	$[Mo_2O(S_2CN((CH_2)_5)_2)_2(N_2CSPh)_2]$	pinkish red	238–240	37.6 (37.8)	3.7 (3.6)	10.0 (10.1)			7.4 m (6) 8.1 m (4)	1.7 m (12), 3.5 (2) 3.8 m (2), 4.06 m (4)
4d	$[Mo_2O(S_2CNEt_2)_2(N_2CSPh)_2]$	red	296–298	36.2 (35.9)	3.8 (3.7)	10.6 (10.5)	24.5 (24.0)	837 (802)	7.45 m (6) 8.2 m (4)	1.08 t (3), 1.22 t (3), 1.36 t (6) 3.44 q (2), 3.69 q (2), 3.96 q (4)
4e	$[Mo_2O(S_2CNEt_2)_2(N_2CSC_6N_4\text{-}p\text{-}OMe)_2]$	red	254–257	35.7 (36.1)	3.9 (3.9)	9.5 (9.7)		895 (862)	7.0 m (4)	1.0–1.4 m (12)
4	$[Mo_2O(S_2CNEt_2)_2(N_2CSC_6H\text{-}p\text{-}Cl)_2]$	red	298–301	33.2 (33.1)	3.3 (3.2)	9.4 (9.6)	24.3 (22.0)	851 (857)		

[a] In °C with decomposition. [b] Calculated values in parentheses. [c] Determined in 1,2-dichloroethane. [d] Contains 1 mol of CH_2Cl_2 of crystallization. [e] Oxygen analysis: found 2.5%; complex **4a** requires 2.0%. [f] In CD_2Cl_2 solution; integrated values in parentheses.

Table III. Final Positional and Thermal Parameters for $[Mo_2O(S_2CNEt_2)_2(C_6H_5CON_2)_2]\cdot CH_2Cl_2$[a]

atom	x	y	z	U_{11} or U	U_{22}	U_{33}	U_{12}	U_{13}	U_{23}
Mo1	0.21055 (9)	−0.3429 (1)	−0.1196 (2)	3.2 (1)	3.9 (2)	3.1 (1)	−0.43 (8)	0.40 (8)	0.69 (9)
Mo2	0.29914 (9)	−0.4498 (1)	−0.3487 (2)	3.2 (1)	3.7 (2)	3.2 (1)	−0.05 (8)	0.64 (8)	0.40 (9)
S1	0.1412 (3)	−0.3436 (5)	0.1035 (5)	5.5 (4)	5.3 (4)	3.1 (4)	−0.26 (3)	1.8 (3)	0.8 (3)
S2	0.2124 (3)	−0.5633 (5)	−0.1062 (5)	6.8 (4)	3.9 (4)	5.4 (4)	−0.8 (3)	2.6 (3)	0.9 (3)
S3	0.2842 (3)	−0.4488 (5)	−0.6009 (6)	3.2 (3)	7.9 (4)	3.4 (4)	−0.7 (3)	0.2 (3)	1.2 (3)
S4	0.4128 (3)	−0.3662 (5)	−0.4097 (5)	3.5 (3)	5.7 (4)	3.6 (4)	−0.8 (3)	0.3 (3)	1.3 (3)
O1	0.8828 (6)	0.2263 (11)	0.1517 (14)	2.4 (7)	3.6 (8)	3.8 (9)	1.1 (6)	1.0 (7)	0.1 (7)
O2	0.7568 (7)	0.1701 (11)	−0.184 (14)	2.3 (7)	3.6 (8)	4.6 (9)	0.8 (6)	1.1 (7)	0.3 (7)
O3	0.6810 (7)	0.6059 (11)	0.3616 (14)	5.1 (9)	2.6 (8)	3.3 (9)	−0.4 (7)	2.1 (7)	−1.0 (7)
N1	0.8693 (8)	0.3363 (14)	0.3872 (16)	3.3 (4)					
N2	0.8110 (8)	0.3939 (13)	0.3261 (16)	3.0 (4)					
N3	0.6395 (8)	0.2361 (14)	0.0704 (16)	2.8 (4)					
N4	0.6838 (7)	0.3383 (12)	0.1471 (15)	2.0 (3)					
N5	0.1344 (9)	0.4180 (16)	0.1185 (19)	5.3 (5)					
N6	0.5857 (9)	0.3896 (15)	0.6910 (18)	4.3 (5)					
C1	0.9070 (11)	0.2498 (19)	0.2864 (21)	3.8 (5)					
C2	0.6847 (10)	0.1543 (17)	−0.0174 (21)	2.9 (5)					
C3	0.1581 (11)	0.4960 (19)	0.0503 (27)	4.6 (6)					
C4	0.3749 (11)	0.5987 (18)	0.4161 (23)	3.9 (6)					
C5	0.4955 (13)	0.6572 (22)	0.3277 (25)	5.8 (7)					
C6	0.4841 (19)	0.8028 (32)	0.3574 (38)	11.5 (11)					
C7	0.3824 (13)	0.5762 (23)	0.1503 (28)	6.4 (7)					
C8	0.4049 (15)	0.4344 (26)	0.0774 (30)	7.9 (8)					
C9	0.1589 (17)	0.7672 (28)	0.0669 (34)	9.5 (9)					
C10	0.1056 (19)	0.2073 (32)	−0.0441 (40)	11.9 (12)					
C11	0.0911 (13)	0.4673 (23)	0.2548 (27)	6.5 (7)					
C12	0.0083 (16)	0.4819 (27)	0.2119 (31)	8.4 (9)					
C13	1.0275 (12)	0.8278 (20)	0.6842 (25)	4.8 (6)					
C14	0.9998 (21)	0.1891 (32)	0.4588 (40)	12.4 (12)					
C15	1.0727 (24)	0.1123 (39)	0.4879 (42)	14.5 (14)					
C16	1.1007 (20)	0.0131 (35)	0.3596 (45)	12.3 (12)					
C17	1.0725 (15)	0.0061 (24)	0.2347 (31)	7.1 (8)					
C18	1.0097 (12)	0.0816 (21)	0.2090 (24)	4.9 (6)					
C19	0.6552 (11)	0.0303 (18)	−0.1185 (22)	3.8 (5)					
C20	0.7054 (13)	−0.0514 (22)	−0.2655 (26)	5.7 (7)					
C21	0.6780 (16)	−0.1648 (27)	−0.3090 (32)	8.5 (9)					
C22	0.6041 (13)	−0.1979 (21)	−0.3017 (26)	5.81 (7)					
C23	0.5560 (12)	−0.1174 (20)	−0.2145 (25)	5.3 (6)					
C24	0.7568 (8)	0.0043 (20)	−0.1147 (24)	4.8 (6)					
Cl1	0.7568 (8)	1.0874 (15)	0.3669 (16)	18.1 (12)	17.4 (12)	32.3 (21)	−5.7 (10)	−12.0 (14)	10.3 (14)
Cl2	0.6580 (11)	0.9101 (20)	0.2014 (21)	25.5 (20)	28.1 (21)	22.8 (19)	−4.9 (16)	0.7 (16)	11.0 (17)
C25	0.7042 (25)	0.9401 (40)	0.2386 (59)	21.1 (15)					

[a] Estimated standard deviations are given in parentheses. The U_{ij} values are $\times 10^3$. The vibrational coefficients relate to the expression $T = \exp[-2\pi^2(U_{11}h^2a^{*2} + U_{22}k^2b^{*2} + U_{33}l^2c^{*2} + 2U_{12}hka^*b^* + 2U_{13}hla^*c^* + 2U_{23}klb^*c^*)]$.

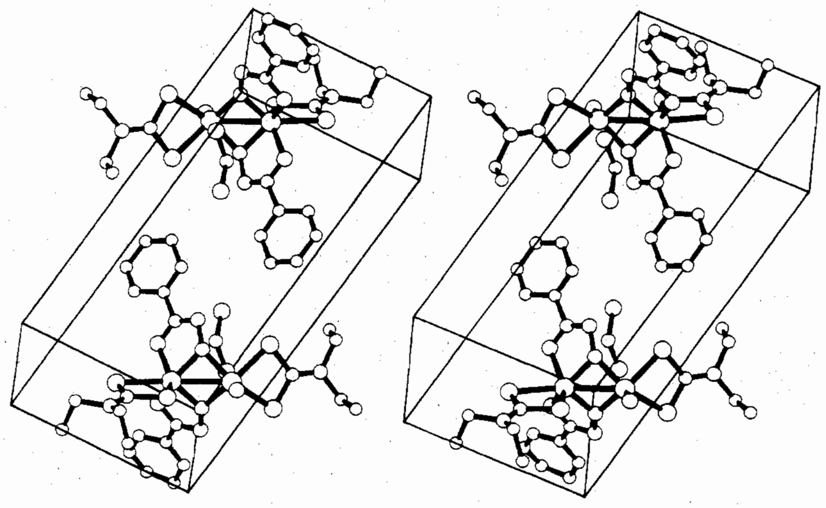

Figure 3. A stereoscopic view of the packing of the symmetry-related $Mo_2O(S_2CNEt_2)_2(C_6H_5CON_2)_2\cdot CH_2Cl_2$ molecules in the unit cell.

as that provided by the benzene dithiolato ligand or the benzoyldiazenido group. The relative importance of the metal electronic configuration and the ligand π-acceptor orbitals in determining the geometry of six-coordinate transition-metal complexes has been discussed.[37] The number of d electrons appears to be of paramount importance[34] although the bite angle of the ligands and their mutual steric interference must influence the observed equilibrium geometry. The assignment of a formal oxidation state in complexes with highly delocalized orbitals is artificial and the actual charge distribution even in the monomeric complexes is far from that assumed in assigning Mo oxidation states. Although the assignment becomes, if anything, more ambiguous for the dimeric compounds **3** and **4**, possessing a delocalized bridge system,

Table IV. Final Positional and Thermal Parameters for $[Mo_2O(S_2CNEt_2)_2(ClC_6H_4CSN_2)_2]\cdot CHCl_3$[a]

atom	x	y	z	U_{11} or U	U_{22}	U_{33}	U_{12}	U_{13}	U_{23}
Mo1	0.2330 (1)	−0.1170 (1)	0.1912 (1)	4.2 (1)	4.2 (1)	4.2 (1)	−0.14 (9)	1.7 (1)	−0.21 (9)
Mo1	0.3466 (1)	0.0249 (1)	0.2826 (1)	4.5 (1)	3.4 (1)	4.5 (1)	−0.18 (9)	2.0 (1)	−0.18 (10)
S1	0.0826 (4)	−0.1769 (5)	0.1207 (4)	4.2 (4)	4.8 (4)	6.9 (5)	−0.48 (34)	1.5 (3)	−0.52 (35)
S2	0.1352 (3)	0.0230 (6)	0.2026 (3)	3.7 (4)	5.7 (4)	6.6 (5)	0.37 (32)	1.6 (2)	−1.7 (4)
S3	0.4684 (3)	−0.0086 (5)	0.3962 (3)	4.3 (4)	4.1 (4)	4.3 (4)	−1.1 (3)	2.0 (3)	0.9 (3)
S4	0.4677 (4)	0.1167 (5)	0.2739 (3)	5.3 (4)	5.3 (4)	4.2 (4)	−1.8 (3)	2.3 (3)	−0.07 (31)
S5	0.2484 (4)	−0.1741 (5)	0.0826 (3)	5.5 (4)	4.1 (4)	4.0 (4)	−0.2 (3)	2.2 (3)	−0.5 (3)
S6	0.2507 (4)	−0.3143 (5)	0.2164 (3)	5.7 (4)	3.9 (4)	4.0 (4)	−0.9 (3)	1.0 (3)	−1.0 (3)
N1	0.3037 (9)	−0.0048 (13)	0.1780 (9)	3.5 (10)	3.4 (11)	5.4 (12)	0.4 (8)	2.3 (9)	0.9 (9)
N2	0.3342 (10)	0.0149 (13)	0.1250 (9)	5.2 (11)	3.2 (11)	3.9 (11)	1.8 (9)	0.4 (10)	0.6 (9)
N3	0.3047 (10)	−0.1255 (14)	0.2924 (9)	4.1 (10)	2.7 (10)	6.1 (12)	−0.01 (88)	3.8 (10)	−0.9 (9)
N4	0.3371 (10)	−0.2149 (15)	0.3400 (9)	4.7 (11)	4.3 (12)	4.0 (11)	1.2 (9)	1.7 (9)	1.9 (10)
N5	−0.0297 (10)	−0.0232 (16)	0.1216 (9)	2.3 (10)	7.1 (14)	5.9 (13)	1.7 (10)	0.3 (9)	−0.05 (11)
N6	0.0978 (11)	0.3783 (16)	0.4029 (10)	5.5 (12)	5.7 (13)	6.7 (13)	2.7 (11)	1.8 (11)	−0.06 (11)
C1	0.0493 (14)	−0.0580 (18)	0.1426 (11)	4.6 (6)					
C2	0.5221 (12)	0.0818 (18)	0.3661 (11)	4.0 (6)					
C3	0.3078 (12)	−0.0578 (16)	0.0750 (10)	3.4 (5)					
C4	0.3111 (11)	−0.3124 (17)	0.3069 (9)	2.7 (5)					
C5	−0.1006 (16)	−0.0979 (23)	0.0720 (14)	7.4 (8)					
C6	−0.1088 (16)	−0.0762 (23)	−0.0032 (14)	7.2 (8)					
C7	−0.0594 (21)	0.0816 (32)	0.1579 (19)	11.7 (12)					
C8	−0.0507 (24)	0.1704 (35)	0.1131 (21)	13.7 (14)					
C9	0.1384 (18)	0.3908 (26)	0.4868 (16)	8.9 (9)					
C10	0.1994 (23)	0.4776 (33)	0.5085 (19)	12.5 (13)					
C11	0.1468 (16)	0.3049 (24)	0.3720 (14)	7.5 (8)					
C12	0.1278 (18)	0.1853 (27)	0.3795 (16)	9.3 (9)					
C13	0.3294 (14)	−0.0569 (19)	0.0103 (2)	5.1 (6)					
C14	0.3793 (15)	0.0316 (21)	0.0041 (13)	6.0 (7)					
C15	0.4041 (17)	0.0374 (25)	−0.0544 (15)	8.2 (8)					
C16	0.3786 (15)	−0.0467 (22)	−0.1030 (13)	6.1 (7)					
C17	0.3303 (16)	−0.1314 (23)	−0.1036 (14)	6.9 (7)					
C18	0.3045 (14)	−0.1402 (20)	−0.0435 (13)	5.9 (7)					
C19	0.3381 (12)	−0.4166 (16)	0.3495 (10)	3.1 (5)					
C20	0.3723 (14)	−0.4168 (19)	0.4268 (20)	5.0 (6)					
C21	0.3988 (14)	−0.5154 (20)	0.4667 (12)	5.6 (7)					
C22	−0.1087 (14)	0.1159 (21)	0.4277 (13)	6.0 (7)					
C23	0.3574 (15)	−0.6195 (22)	0.3524 (13)	6.4 (7)					
C24	0.3274 (14)	−0.5195 (20)	0.3143 (12)	5.2 (6)					
C25	0.5456 (20)	0.7478 (29)	0.3238 (18)	10.8 (10)					
Cl1	−0.4140 (6)	0.0439 (8)	0.1746 (4)	12.7 (7)	13.9 (8)	8.4 (6)	3.9 (6)	7.5 (5)	2.9 (6)
Cl2	−0.0754 (5)	0.2389 (6)	0.4774 (4)	13.3 (7)	4.1 (4)	8.9 (6)	−1.5 (4)	3.1 (5)	−2.2 (4)
Cl3	0.5474 (8)	0.6027 (9)	0.3314 (6)	24.4 (13)	9.7 (8)	14.2 (9)	3.2 (9)	10.1 (9)	0.7 (7)
Cl4	0.6377 (6)	0.8095 (14)	0.3500 (7)	7.5 (6)	30.0 (17)	17.3 (11)	−4.6 (9)	6.4 (7)	−4.8 (11)
Cl5	0.4751 (5)	0.7927 (8)	0.2414 (4)	10.8 (7)	13.6 (8)	7.6 (6)	3.9 (6)	3.7 (5)	−0.2 (5)

[a] Estimated standard deviations are given in parentheses. The U_{ij} values are $\times 10^3$. The vibrational coefficients relate to the expression $T = \exp[-2\pi^2(U_{11}h^2a^{*2} + U_{22}k^2b^{*2} + U_{33}l^2c^{*2} + 2U_{12}hka^*b^* + 2U_{13}hla^*c^* + 2U_{23}klb^*c^*)]$.

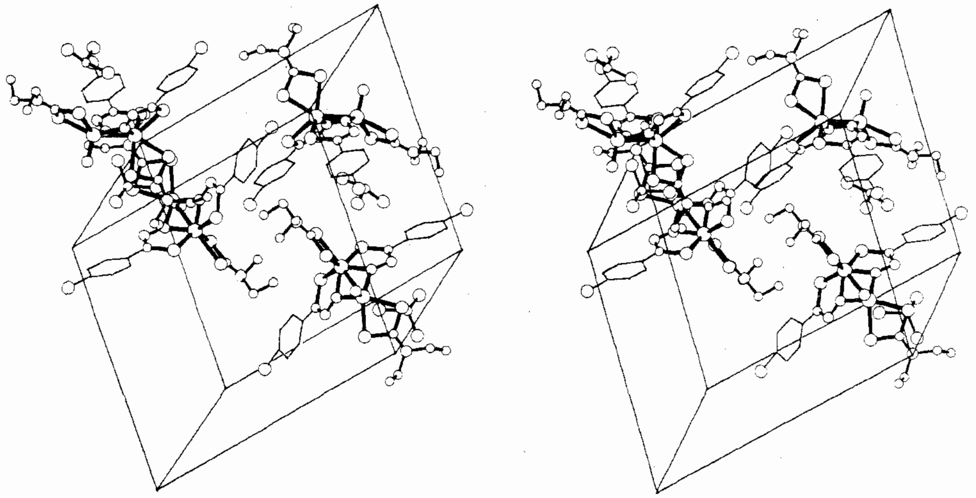

Figure 4. A stereoscopic view of the packing of the symmetry-related $Mo_2O(S_2CNEt_2)_2(ClC_6H_4CSN_2)_2\cdot CHCl_3$ molecules in the unit cell.

there may be some heuristic value in considering the Mo oxidation states. Arbitrarily assuming that the benzoyldiazenido or thiobenzoyldiazenido ligands behave as ligating trinegative anions and the dithiocarbamato ligands as mononegative, the complexes may be viewed in terms of two d^1 Mo(V) species, spin-paired through the bridge framework. Alternatively, the complexes may be assigned as mixed valence species in which the Mo1 site is formally d^0 Mo(VI) and the

Table V. Intramolecular Bond Distances (in Å) for $[Mo_2O(S_2CNEt_2)_2(C_6H_5CON_2)_2]\cdot CH_2Cl_2$

Mo1–Mo2	2.662 (2)	N5–C3	1.32 (3)
Mo1–O1	2.05 (1)	N6–C4	1.31 (3)
Mo1–O2	2.04 (1)	N3–N4	1.40 (2)
Mo1–N2	1.92 (1)	N3–C2	1.27 (2)
Mo1–N4	1.89 (1)	O2–C2	1.29 (2)
Mo1–S1	2.524 (6)	C19–C2	1.50 (2)
Mo1–S2	2.420 (6)	N1–N2	1.35 (2)
Mo2–O3	1.66 (1)	N1–C1	1.29 (2)
Mo2–N2	1.97 (1)	O1–C1	1.30 (3)
Mo2–N4	1.97 (1)	C13–C1	1.43 (3)
Mo2–S3	2.435 (6)	S1···S2 (bite)	2.839 (7)
Mo2–S4	2.426 (6)	S3···S4 (bite)	2.861 (7)
S1–C3	1.65 (2)	O1···N2	2.37 (2)
S2–C3	1.74 (2)	O2···N4	2.35 (2)
S3–C4	1.70 (2)	N2···N4	2.74 (2)
S4–C4	1.71 (2)	C–C (av rings)	1.38 (3)
			1.39 (3)
		C25–Cl1	1.70 (9)
		C25–Cl2	1.75 (9)

Table VI. Intramolecular Bond Angles (in deg) for $[Mo_2O(S_2CNEt_2)_2(C_6H_5CON_2)_2]\cdot CH_2Cl_2$

Mo2–Mo1–S1	154.2 (2)	Mo1–N4–Mo2	87.1 (5)
Mo2–Mo1–S2	84.5 (2)	Mo1–O1–C1	115.2 (11)
Mo2–Mo1–N2	47.8 (4)	O1–C1–N1	119.0 (18)
Mo2–Mo1–N4	47.6 (4)	O1–C1–C13	117.9 (17)
Mo2–Mo1–O1	115.9 (4)	N1–C1–C13	123.0 (20)
Mo2–Mo1–O2	115.1 (4)	C1–N1–N2	109.4 (16)
S1–Mo1–S2	70.1 (2)	Mo1–N2–N1	122.9 (10)
O1–Mo1–O2	82.0 (5)	Mo2–N2–N1	141.2 (13)
N2–Mo1–N4	92.0 (6)	Mo1–O2–C2	114.5 (10)
S1–Mo1–N2	135.8 (5)	O2–C2–N3	122.0 (15)
S1–Mo1–N4	130.1 (5)	O2–C2–C19	118.1 (14)
S1–Mo1–O1	84.4 (4)	N3–C2–C19	119.8 (16)
S1–Mo1–O2	81.7 (4)	C2–N3–N4	105.7 (14)
S2–Mo1–N2	93.9 (4)	Mo1–N4–N3	124.4 (9)
S2–Mo1–N4	98.5 (5)	Mo2–N4–N3	139.2 (12)
S2–Mo1–O1	127.5 (4)	Mo1–S1–C3	87.4 (8)
S2–Mo1–O2	134.7 (4)	Mo1–S2–C3	88.9 (8)
O1–Mo1–N2	73.3 (5)	S1–C3–N5	124.5 (16)
O1–Mo1–N4	131.7 (6)	S2–C3–N5	122.0 (14)
O2–Mo1–N2	130.1 (6)	S1–C3–S2	113.5 (14)
O2–Mo1–N4	72.2 (4)	C3–N5–C9	120.9 (19)
Mo1–Mo2–S3	131.3 (1)	C3–N5–C11	122.6 (17)
Mo1–Mo2–S4	127.7 (1)	C9–N5–C11	116.1 (21)
Mo1–Mo2–O3	107.9 (5)	Mo2–S4–C4	86.6 (8)
Mo1–Mo2–N2	46.1 (4)	Mo2–S3–C4	86.7 (8)
Mo1–Mo2–N4	45.2 (4)	S3–C4–N6	124.8 (16)
S3–Mo2–S4	72.1 (2)	S4–C4–N6	121.2 (15)
N2–Mo2–N4	88.1 (5)	S3–C4–S4	114.0 (13)
S3–Mo2–O3	104.2 (5)	C4–N6–C5	124.0 (17)
S3–Mo2–N2	87.8 (5)	C4–N6–C7	122.3 (17)
S3–Mo2–N4	143.6 (5)	C5–N6–C7	113.7 (18)
S4–Mo2–O3	108.3 (5)	N5–C9–C10	107.0 (24)
S4–Mo2–N2	137.0 (5)	N5–C11–C12	107.1 (20)
S4–Mo2–N4	86.8 (4)	N6–C5–C6	105.0 (20)
O3–Mo2–N2	113.4 (6)	N6–C7–C8	107.3 (21)
O3–Mo2–N4	110.6 (6)	C–C–C(ring)	120.0 (20)
Mo1–N2–Mo2	86.2 (6)		119.9 (27)

Table VII. Intramolecular Bond Distances (in Å) for $[Mo_2O(S_2CNEt_2)_2(ClC_6H_4CSN_2)_2]\cdot CHCl_3$

Mo1–Mo2	2.680 (2)	N6–C2	1.31 (2)
Mo1–S1	2.518 (6)	N6–C9	1.55 (3)
Mo1–S2	2.455 (7)	N6–C11	1.52 (4)
Mo1–S5	2.402 (7)	C9–C10	1.42 (5)
Mo1–S6	2.393 (6)	C11–C12	1.48 (4)
Mo1–N1	1.90 (2)	S5–C3	1.77 (2)
Mo1–N3	1.91 (2)	C13–C3	1.49 (4)
Mo2–O1	1.67 (1)	N2–C3	1.26 (2)
Mo2–N1	1.96 (2)	N2–N1	1.39 (3)
Mo2–N3	1.97 (2)	S6–C4	1.69 (2)
Mo2–S3	2.438 (5)	C19–C4	1.47 (3)
Mo2–S4	2.436 (7)	N4–C4	1.32 (3)
S1–C1	1.65 (2)	N4–N3	1.39 (2)
S2–C1	1.77 (2)	S1···S2 (bite)	2.825 (9)
N5–C1	1.33 (3)	S3···S4 (bite)	2.871 (9)
N5–C5	1.52 (3)	S5···N1	2.68 (2)
N5–C7	1.63 (5)	S6···N3	2.66 (2)
C5–C6	1.48 (4)	N1···N3	2.71 (3)
C7–C8	1.43 (6)	C–C (av rings)	1.39 (4)
S3–C2	1.69 (2)		1.40 (4)
S4–C2	1.76 (2)	C25–Cl3	1.73 (3)
		C25–Cl4	1.65 (4)
		C25–Cl5	1.70 (3)

Table VIII. Intramolecular Bond Angles (in deg) for $[Mo_2O(S_2CNEt_2)_2(ClC_6H_4CSN_2)_2]\cdot CHCl_3$

Mo2–Mo1–S1	150.7 (2)	Mo1–N3–Mo2	87.3 (7)
Mo2–Mo1–S2	81.6 (1)	Mo1–S5–C3	98.2 (8)
Mo2–Mo1–S5	118.7 (2)	S5–C3–C13	116.3 (14)
Mo2–Mo1–S6	118.4 (1)	S5–C3–N2	120.1 (18)
Mo2–Mo1–N1	46.9 (5)	C13–C3–N2	123.4 (20)
Mo2–Mo1–N3	47.3 (5)	C3–N2–N1	111.6 (17)
S1–Mo1–S2	69.2 (2)	Mo1–N1–N2	134.1 (12)
S5–Mo1–S6	82.2 (2)	Mo2–N1–N2	133.9 (12)
N1–Mo1–N3	90.4 (7)	Mo1–S6–C4	100.7 (7)
S1–Mo1–S5	83.1 (2)	S6–C4–C19	121.9 (14)
S1–Mo1–S6	81.8 (2)	S6–C4–N4	119.3 (15)
S1–Mo1–N1	134.5 (5)	C19–C4–N4	118.8 (15)
S1–Mo1–N3	131.6 (6)	C4–N4–N3	111.3 (14)
S2–Mo1–S5	127.8 (2)	Mo1–N3–N4	134.5 (11)
S2–Mo1–S6	132.8 (3)	Mo2–N3–N4	133.1 (12)
S2–Mo1–N1	92.7 (6)	Mo1–S1–C1	90.1 (8)
S2–Mo1–N3	96.5 (6)	Mo1–S3–C1	89.5 (8)
S5–Mo1–N1	75.9 (6)	S1–C1–S2	111.0 (13)
S5–Mo1–N3	133.6 (6)	S1–C1–N5	127.5 (16)
S6–Mo1–N1	133.0 (5)	S2–C1–N5	121.5 (17)
S6–Mo1–N3	75.6 (5)	C1–N5–C5	119.0 (20)
Mo1–Mo2–S3	131.2 (2)	C1–N5–C7	124.7 (18)
Mo1–Mo2–S4	130.5 (2)	C5–N5–C7	115.0 (20)
Mo1–Mo2–O1	106.0 (4)	N5–C5–C6	106.7 (26)
Mo1–Mo2–N1	45.2 (5)	N5–C7–C8	98.6 (32)
Mo1–Mo2–N3	45.4 (4)	Mo2–S3–C2	87.4 (6)
S3–Mo2–S4	72.2 (2)	Mo2–S4–C2	86.0 (8)
N1–Mo2–N3	87.1 (7)	S3–C2–S4	113.0 (10)
S3–Mo2–O1	105.8 (4)	S3–C2–N6	127.0 (16)
S4–Mo2–O1	106.2 (5)	S4–C2–N6	119.9 (18)
S3–Mo2–N1	141.8 (5)	C2–N6–C9	119.3 (22)
S3–Mo2–N3	88.4 (4)	C2–N6–C11	125.4 (19)
S4–Mo2–N1	88.2 (5)	C4–N6–C11	114.8 (18)
S4–Mo2–N3	141.1 (5)	N6–C4–C10	111.0 (28)
O1–Mo2–N1	111.1 (6)	N6–C11–C12	109.0 (26)
O1–Mo2–N3	111.5 (7)	C–C–C(rings)	120.0 (22)
Mo1–N1–Mo2	87.9 (8)		120.0 (22)

Mo2 site d^2 Mo(IV). Some support for the latter assignment is rendered by the Mo–N bond lengths which average 1.91 (2) Å for the Mo–N and 1.97 (2) Å for Mo2–N in both structures **3** and **4**, consistent with the larger covalent radius of Mo(IV). Likewise, the geometry of the coordination polyhedron at Mo1 argues for a metal center with few d electrons and the geometry at Mo2 is common to that found for a number of Mo(IV) sites.[12,38]

Although the bond length difference is statistically significant and the coordination polyhedra of the two Mo sites unique, the large steric hindrances in the edge-sharing coordination polyhedra (Figure 5) make any conclusions tenuous at best. Further support for the mixed-valence assignment comes from the electrochemical investigations (vide infra) where substitution of the sulfur donor atoms in **4** for the oxygen donors in **3** results in a redox potential 0.3 V more positive for the first cathodic couple. Again, the delocalized nature of the diazenido ligands, the close contact of the Mo atoms in the bridged geometry (2.66 Å), and the major distortions of the coordination polyhedra preclude a definitive statement in the absence of a detailed molecular orbital study of the dimers.

An unusual feature of the coordination geometry at Mo1 is the significantly longer bond length of 2.52 Å (av) for Mo1–S1 in both structures, as compared to 2.44 Å (av) for the Mo–S bond lengths to the other sulfur donors of the

Table IX. Equations of Least-Squares Planes in $[Mo_2O(S_2CNEt_2)_2(C_6H_5CON_2)_2]\cdot CH_2Cl_2$ and $[Mo_2O(S_2CNEt_2)_2(ClC_6H_4CSN_2)_2]\cdot CHCl_3$

(a) $[Mo_2O(S_2CNEt_2)_2(C_6H_5CON_2)_2]\cdot CH_2Cl_2$

atom	dist from plane, Å	atom	dist from plane, Å
Plane 1: $-2.163X + 10.6055Y - 2.4609Z - 1.6723 = 0$			
S3	0.063 (6)	N4	−0.07 (2)
S4	−0.064 (6)	Mo2	0.72
N2	0.07 (2)		
Plane 2: $2.4037X - 7.3959Y + 8.4659Z - 0.3898 = 0$			
N1	0.00 (1)	O1	0.03 (1)
N2	0.01 (1)	Mo1	−0.017 (2)
C1	−0.02 (2)		
Plane 3: $3.8902X - 7.4995Y + 8.1126Z - 1.3307 = 0$			
C13	0.05 (2)	C16	0.03 (2)
C14	−0.02 (2)	C17	−0.01 (2)
C15	−0.02 (2)	C18	−0.03 (2)
Plane 4: $2.4037X - 7.3959Y + 8.4659Z + 0.3898 = 0$			
N3	−0.00 (1)	O2	−0.01 (1)
N4	−0.01 (1)	Mo1	0.009 (2)
C2	0.01 (1)		
Plane 5: $11.735X + 8.6091Y - 3.4535Z - 11.8205 = 0$			
C19	−0.02 (2)	C22	−0.05 (2)
C20	−0.01 (2)	C23	0.02 (2)
C21	0.04 (2)	C24	0.02 (2)

(b) $[Mo_2O(S_2CNEt_2)_2(ClC_6H_4CSN_2)_2]\cdot CHCl_3$

atom	dist from plane, Å	atom	dist from plane, Å
Plane 6: $11.6185X - 8.5436Y - 8.9251Z - 1.9858 = 0$			
S3	−0.007 (4)	N3	0.007 (8)
S4	0.007 (4)	Mo2	−0.69
N1	−0.007 (8)		
Plane 7: $11.4847X - 6.3096Y + 4.3594Z + 4.2728 = 0$			
N1	0.014 (8)	S5	0.038 (4)
N2	0.028 (8)	Mo1	−0.025 (2)
C3	−0.05 (2)		
Plane 8: $11.3291X - 6.2919Y + 4.6616Z + 4.1154 = 0$			
C13	0.03 (1)	C17	−0.04 (1)
C14	−0.00 (1)	C18	0.01 (1)
C15	−0.03 (1)	Cl1	0.038 (8)
C16	−0.01 (1)		
Plane 9: $16.9791X - 0.1485Y - 11.7992Z + 1.7310 = 0$			
N3	0.08 (8)	S6	0.020 (4)
N4	0.013 (8)	Mo1	−0.013 (1)
C4	−0.03 (1)		
Plane 10: $17.2121X + 1.5579Y - 7.9821Z - 2.3558 = 0$			
C19	0.02 (1)	C23	−0.01 (1)
C20	−0.00 (1)	C24	0.00 (1)
C21	−0.03 (1)	Cl2	0.000 (2)
C22	0.02 (1)		

(c) Selected Dihedral Angles between Least-Squares Planes

plane A	plane B	angle, deg	plane A	plane B	angle, deg
2	3	5.4	7	8	0.88
2	4	119.2	7	9	122.9
3	5	116.6	8	10	125.5
4	5	0.74	9	10	14.8

dithiocarbamate ligands. This Mo–S bond is nearly trans to the Mo–Mo vector, and the significant lengthening in both structures may suggest a trans influence.

Although the origin of this effect is not clear, steric interactions and/or metal–metal bonding may play a significant role. Steric hindrances between chelating groups in **4**, as demonstrated by short S···S contact distances (Figure 5) and the deformation from regular trigonal prismatic geometry of the Mo1 valence angles, and the low overall symmetry of the Mo1 sites must be taken into account. However, the consistency of the Mo1–S1 bond distances in both **4** and **3**, where substitution of oxygen donor groups for sulfur in the diazenido ligand may be expected to diminish substantially the valence shell steric interactions, argues that steric contributions are not the dominant factor. Certainly, the short Mo1–Mo2 distances and the acute Mo1–N–Mo2 angles in both structures suggest considerable metal–metal interaction, although the nature of the metal–metal overlap (direct σ or π bonding) is not apparent in the absence of detailed theoretical considerations.

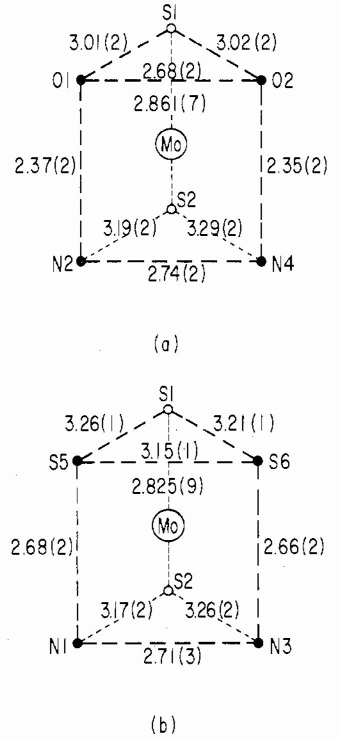

Figure 5. Schematic representation of the distorted trigonal prismatic geometry (a) about Mo1 in $Mo_2O(S_2CNEt_2)_2(PhCON_2)_2$ and (b) about Mo1 in $Mo_2O(S_2CNEt_2)_2(ClC_6H_4CSN_2)_2$.

Recent theoretical studies[39] of the relatively simple M_2L_6 transition-metal dimers show that the interrelationship and relative importance of a number of factors must be considered and that direct metal–metal overlap may not be the sole cause of a low-spin ground state or short metal–metal distances. The situation is somewhat more ambiguous for the highly asymmetric dimers of this study which are not amenable to discussions based on simple symmetry-based molecular orbital arguments. The metal–metal distance, the constrained Mo_2N_2 bridge, and the close contact of the syn donors to the Mo atoms (S2–O3 = 3.06 Å in **3** and S2–O1 = 2.90 Å in **4**, as compared to 3.87 Å for the syn O···O contact in the cis-bent structure $Mo_2O_2S_2(S_2C_2(CN)_2)_2^{2-}$ [23]) argue for a strong metal–metal interaction although the nature of bonding remains problematical.

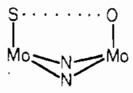

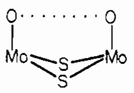

The benzoyldiazenido ligand in **3** and the thiobenzoyldiazenido group in **4** are coordinated in both a chelating and bridging mode, the terminal nitrogen atoms of each functioning as the bridging group. In both structures the Mo_2N_2 rhombus is nonplanar, the angle between the two Mo–N2–N4 planes in **3** is 150.9° while that between Mo–N1–N3 planes in **4** is

Table X. Structural Parameters for Square-Pyramidal Molybdenum Complexes or Fragments with Apical Oxo Groups, $MoOL_4$[a]

complex	Mo-Mo	Mo-O_t	Mo-L	Mo displacement,[b] Å	Ref
$[Mo_2O(S_2CNEt_2)_2(C_6H_5CON_2)_2]\cdot CH_2Cl_2$, Mo2	2.662 (2)	1.66 (1)	2.431 (6), S, av 1.97 (1), N, av	0.72	*c*
$[Mo_2O(S_2CNEt_2)_2(ClC_6H_4CSN_2)_2]\cdot CHCl_3$, Mo2	2.680 (2)	1.67 (1)	2.437 (6), S, av 1.971 (1), N, av	0.69	*c*
$[Mo_2O_4(S_2CNEt_2)_2]$	2.580 (1)	1.678 (2)	2.455 (3), S, av 1.941 (1), O, av	0.74	18
$[MoO(S_2CNPr_2)_2]$		1.664 (8)	2.413 (5), S, av	0.83	12
$[(C_4H_9)_4N]_2[Mo_2O_2S_2[S_2C_2(CN)_2]_2]$	2.821 (2)	1.664 (7), av	2.434 (3), S, av 2.206 (3), S_b, av	0.72	23
$[MoO(S_2CS\text{-}i\text{-}C_3H_7)_2]$		1.66 (1)	2.446 (4), S, av 2.370 (4), S, av	0.86	38

[a] Abbreviations: S, S donor from terminal ligand; S_b, bridging sulfido group; O_t, apical oxo group. [b] Displacement from the plane generated by the ligands L_4 in the direction of the apical oxo group, O_t. [c] This work.

Table XI. Ideal and Observed Angles for ML_6 Complexes

complex	dihedral angles,[a] deg δ_1	δ_2	δ_3	angle of twist,[b] deg
ideal octahedral[c]	70.5, 70.5, 70.5	70.5, 70.5, 70.5	70.5, 70.5, 70.5 70.5, 70.5, 70.5	60.0
$Mo_2O(S_2CNEt_2)_2(C_6H_5CON_2)_2\cdot CH_2Cl_2$	1.9, 5.2, 8.3	111.6, 112.6, 124.9	82.5, 86.8, 88.8 86.5, 88.5, 88.7	10.8
$Mo_2O(S_2CNEt_2)_2(ClC_6H_4CSN_2)_2$	0.6, 2.4, 11.2	112.5, 117.7, 123.4	85.6, 86.8, 88.5 85.0, 87.1, 89.9	4.3
ideal MoS_4N_2, C_s[d]	0.0, 6.1, 6.1	115.9, 124.0, 124.0	85.4, 90.0, 90.0 85.4, 90.0, 90.0	0.0
ideal trigonal prism, D_{3h}[c]	0, 0, 0	120, 120, 120	90, 90, 90 90, 90, 90	0.0

[a] The dihedral angles, δ_1, δ_2, and δ_3 are those defined in ref 50. For trigonal-prismatic geometry, the δ_1's define the rectangular or square faces, the δ_2's define the angles between the rectangular faces, and the δ_3's are the dihedral angles between the rectangular faces and the triangular faces of the prism. [b] The twist angles were calculated by taking the average of the projection angles on the plane normal to the line generated through the metal and the centroid of the top and bottom triangular faces. [c] Dihedral angles for the octahedron and the ideal trigonal prism are given in ref 50. [d] The idealized geometry "MoS_4N_2" is based on the polyhedron generated about the Mo atom by chelating ligands having the following shape-determining parameters: S···S (bite), 2.75 Å; S···N (bite), 2.76 Å; S···S edge-non-bonding distances, 3.20 Å; S···N edge-non-bonding distances, 3.10 Å.

151.5°. The bond lengths in the Mo–N–N–C–O and Mo–N–N–C–S ring systems, which are intermediate between single and double bonds, the valence angles at the ring atoms, and the planarity of five-membered chelate rings (Table IX) suggest considerable delocalization.

The geometry of the dithiocarbamate ligands is unexceptional and similar to that observed for previously reported Mo–[12,18,19] and other transition metal–dithiocarbamate complexes.[40–42,44] The short exocyclic C–N bond length (1.30–1.33 Å) suggests that resonance form **7** makes a significant contribution to the overall electronic structure of the ligand.[41,43]

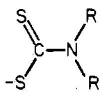
5

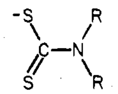
6

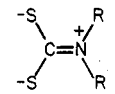
7

An unusual feature of the dithiocarbamate geometry in compounds **3** and **4** is the nonequivalence of the C–S1 and C–S2 bond lengths for the ligand coordinated to the trigonal-prismatic Mo1. In both cases the significant differences in the C–S bond lengths (0.09 and 0.12 Å for **3** and **4**, respectively) correlate with the long–short Mo1–S1 and Mo1–S2 bond lengths, previously discussed. This significant C–S asymmetry suggests greater double bond character for C3–S1 in **3** and C1–S1 in **4** as compared to the C3–S2 and C1–S2 bond lengths. The increased double bond character appears to be related to the Mo–S1 bond distances which are unusually long (2.524 (6) and 2.518 (6) Å) indicating that the C–S interaction builds at the expense of the Mo–S interaction. Similar trends in metal–sulfur and sulfur–carbon bond lengths have been observed for the tin dithiocarbamates.[45–47]

Table XII. Intermolecular Contact Distances between the Complex Molecule and the Molecule of Solvolysis (Å)

(a) $[Mo_2O(S_2CNEt_2)_2(C_6H_5CON_2)_2]\cdot CH_2Cl_2$

Cl1···Mo1	4.25 (2)	Cl1···N1	3.42 (2)
Cl1···Mo2	4.01 (2)	Cl1···N2	3.66 (2)
Cl1···C2	4.11 (3)	Cl1···C1	3.53 (3)
Cl1···S3	3.88 (2)	Cl2···C19	3.66 (3)
Cl1···S4	3.99 (2)	Cl2···C20	3.69 (3)
Cl1···O1	3.79 (2)		

(b) $[Mo_2O(S_2CNEt_2)_2(ClC_6H_4CSN_2)_2]\cdot CHCl_3$

Cl3···C2	4.02 (2)	Cl5···Mo1	4.05 (1)
Cl3···S2	3.80 (2)	Cl5···Mo2	3.85 (1)
Cl3···N5	3.99 (2)	Cl5···S3	3.95 (1)
Cl3···C1	3.84 (2)	Cl5···S4	3.92 (1)
Cl3···C12	3.67 (1)	Cl5···S5	3.96 (1)
Cl4···C1	4.29 (2)	Cl5···S6	3.93 (1)
Cl4···C2	4.13 (2)	Cl5···N1	3.64 (2)
Cl4···S5	3.92 (2)	Cl5···N2	3.71 (2)
Cl4···N4	3.73 (3)	Cl5···N3	3.64 (2)
Cl4···C4	3.45 (1)	Cl5···N4	3.68 (3)
Cl4···C19	3.70 (1)	Cl5···C3	3.87 (1)
		Cl5···C4	3.80 (1)

A final structural feature of interest is the presence in both **3** and **4** of the chlorinated hydrocarbon solvent molecule occupying the molecular cavity formed by the planes of the benzoyldiazenido and thiobenzoyldiazenido ligands. The importance of the size and nature of the solvent molecule is reflected in the failure of the attempts to produce suitable crystals from a number of nonchlorinated organic solvents. In both compounds, one Cl atom of the solvent molecule is directed toward the Mo1–Mo2 vector, resulting in a number of close contacts as shown in Table XII. The approach to the coordinatively unsaturated Mo2 atom is particularly close, 4.01 (2) and 3.85 (1) Å in **3** and **4**, respectively, as compared to

Table XIII. Electrochemistry[a] of the Complexes $[Mo_2O(PhCYNN)_2(S_2CNEt_2)_2]$[b]

	normal-pulse voltammetry			ac voltammetry			cyclic voltammetry		
complex	$E_{1/2}$, V	$E_{3/4} - E_{1/4}$, mV	i_l/C, μA M^{-1}	E_p, V	$\Delta E_{1/2}$, mV	i_p/C, μA M^{-1}	i_p^c/i_p^a	ΔE_p,[c] mV	$i_p^f/C\nu^{1/2}$, μA $s^{1/2}$ M^{-1} $mV^{-1/2}$
$[Mo_2O(PhCON_2)_2(S_2CNEt_2)_2]$	−1.35	53	166	−1.32	92	58	1.0	61	7.4
	−1.92	82	174	−1.98	134	63	*d*		8.0
$[Mo_2O(PhCSN_2)_2(S_2CNEt_2)_2]$	−1.07	52	153	−1.06	91	57	1.0	63	7.2
	−1.62	85	166	−1.62	125	59	*d*		7.4

[a] Potentials vs. saturated calomel electrode for a system 0.1 M in $[Bu_4N]PF_6$, 0.5 mM in complex, CH_2Cl_2 solvent; three-electrode configuration with a platinum working electrode. Analogous results were observed at a hanging mercury drop electrode and a vitreous carbon electrode. [b] Y = O, S. [c] Scan rate 200 mV/s. [d] No anodic process observable at scan rates ranging from 50 to 2000 mV/s.

ca. 3.9 Å for the sum of the van der Waals radii.[43,48] The position of the solvent molecules may also influence the planarity of the benzoyldiazenido and thiobenzoyldiazenido ligands. Examination of Table IX shows that in either complex the dihedral angle between the phenyl residue and the chelate ring system deviates considerably from planarity for one ligand whereas the second exhibits near planarity, consistent with the delocalized electronic structure of the ligand: complex **3** exhibits dihedral angles of 5.4° between planes 2 and 3 and 0.7° between 4 and 5, while the torsion angles between planes 9 and 10 and planes 7 and 8 in compound **4** are 14.8 and 0.9°, respectively. Since there are no apparent intramolecular contacts shorter than 3.8 Å which could account for the observed deviations from planarity, the close intermolecular contacts of the ring carbons with C12 of the methylene chloride solvent molecule in **3** and with C14 of the chloroform molecule in **4** may cause the shift of the phenyl groups from the plane of the chelate ring. The resultant loss of delocalization throughout the ligand groups is reflected in the chelate-carbon phenyl ring–carbon bond distances: C1–C13, 1.43 (3) Å, vs. C2–C19, 1.50 (2) Å, in **3** and C3–C13, 1.44 (3) Å, vs. C4–C19, 1.49 (3) Å, in **4**.

Electrochemical Studies. The results of the voltammetric investigations are presented in Table XIII and typical voltammograms are presented in Figure 6. The initial cathodic process in the complexes is found to be a reversible one-electron transfer. The ratio between the cathodic and anodic peaks i_p^c/i_p^a in the cyclic voltammograms remained near unity for sweep rates ν between 10 and 2000 mV s^{-1}. The separation between cathodic and anodic peak potentials, ΔE_p, ranged from 59 to 61 mV for the various derivatives. As the sweep rate decreased from 200 mV s^{-1}, ΔE_p remained constant. The charge-transfer process is thus reversible in methylene chloride.

The subsequent electron transfer is totally irreversible. No anodic process was observed at scan rates ranging from 50 to 200 mV s^{-1}. These results are consistent with eq 1 for the cathodic processes

$$[Mo_2O(S_2CNEt_2)_2(C_6H_4CSN_2)_2] \underset{e^-}{\overset{-1.06\ V}{\rightleftharpoons}} [Mo_2O(S_2CNEt_2)_2(C_6H_4CSN_2)_2]^- \xrightarrow[e^-]{-1.62\ V} [Mo_2O(S_2CNEt_2)_2(C_6H_4CSN_2)_2]^{2-} \xrightarrow{k_r} \text{“X”} \quad (1)$$

where X is a decomposition product.

A particularly interesting feature of the electrochemical behavior of these complexes is the shift in the redox potentials of the cathodic processes by some 0.30 V to more positive potentials upon replacement of oxygen by sulfur. This suggests a lowering in the energy of the lowest unoccupied molecular orbital by ca. 23 kJ mol^{-1}.

Subsequent voltammograms of solutions electrolyzed at potentials more negative than that observed for the second cathodic processes indicate that the decomposition product “X” is itself electrochemically active giving rise to anodic processes at +0.01 V in the oxygen derivative and −0.46 V in the sulfur complex (Figure 6).

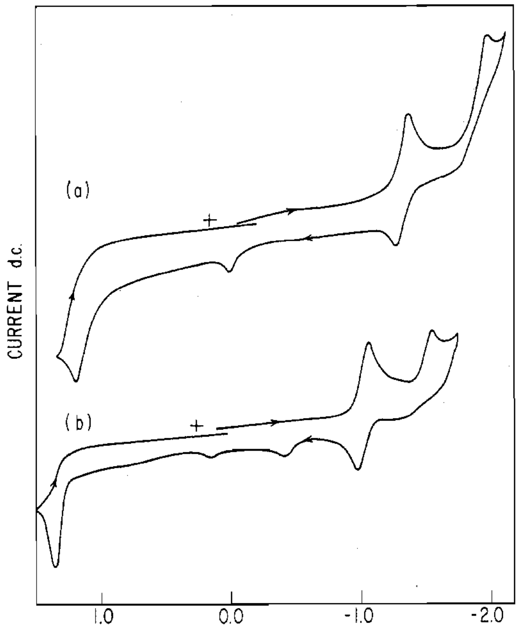

Figure 6. Cyclic voltammograms of (a) 10^{-3} M $Mo_2O(S_2CNEt_2)_2(C_6H_5CON_2)_2$ and (b) 10^{-3} M $Mo_2O(S_2CNEt_2)_2(ClC_6H_4CSN_2)_2$ in 0.1 M TBAHFP in CH_2Cl_2; scan rate was 200 mV s^{-1}.

In an attempt to identify the nature of the dimer orbital involved in the reversible redox processes observed for derivatives **3** and **4d**, a methylene chloride solution of each complex was exhaustively electrolyzed at a platinum mesh working electrode at a potential 0.05 V more negative than the principal cathodic process. In both cases the current–time curve was consistent with a value of $n = 1$. An aliquot of the exhaustively electrolyzed solution was removed, transferred to an EPR tube, and immediately frozen in liquid nitrogen. The EPR spectra of these electrochemically generated species $[Mo_2O(S_2CNEt_2)_2(PhCXN_2)_2]^-$ with X = O and S, were recorded at 77 K and compared to those for monomeric molybdenum complexes displaying square-pyramidal and distorted trigonal-prismatic geometries. The results are presented in Table XIV and a typical EPR spectrum, that observed for $[Mo_2O(S_2CNEt_2)_2(PhCON_2)_2]^-$, is presented in Figure 7.

The rhombic **g** tensors observed for the frozen glass spectra of the monoanions of **3** and **4d** are consistent with the low overall symmetry of these complexes. Although the monomeric distorted trigonal-prismatic complexes investigated in this study exhibit significantly different EPR spectra from those observed for the dimers—isotropic **g** tensors consistent

Table XIV. Electron Paramagnetic Resonance Data[a] for Molybdenum Complexes in Distorted Trigonal-Prismatic and Square-Pyramidal Geometries

complex	geometry[b]	*g* values
$[Mo_2O(S_2CNEt_2)_2(PhCON_2)_2]^-$	Mo1, tp Mo2, sq pyr	$g_1 = 1.97, g_2 = 1.90, g_3 = 1.82$
$[Mo_2O(S_2CNEt_2)_2(PhCSN_2)_2]^-$	Mo1, tp Mo2, sq pyr	$g_1 = 2.02, g_2 = 1.87, g_3 = 1.83$
$[Mo(CH_3C_6H_4CSN_2H)_3]^{-}$ [d]	tp	$g_{iso} = 1.96$
$[Mo(CH_3C_6H_4CSN_2H)_2(CH_3C_6H_4CSNHNC(CH_3)_2)]^{-}$ [e]	*c*	$g_{iso} = 2.01$
$[MoO(S_2CSC_3H_7)_2]^{-}$ [f]	sq pyr	$g_1 = 1.99, g_2 = 1.91, g_3 = 1.84$

[a] Spectra recorded at 77 K on a Varian E-4 spectrophotometer. Although the desirability of variable-temperature studies is recognized,[61] the facilities were not available at the time of this study. More detailed EPR studies are currently being performed. [b] Abbreviations: tp, trigonal prismatic or distorted trigonal prismatic; sq pyr, square pyramidal. [c] The geometry of the parent species is intermediate between octahedral and trigonal-prismatic geometry. A detailed description of the structure is forthcoming. [d] J. Chatt, J. R. Dilworth, K. Venkatasubramian, and J. Zubieta, *J. Chem. Soc., Dalton Trans.*, in press. [e] J. Chatt, J. R. Dilworth, P. Vella and J. Zubieta, unpublished results. [f] Reference 38.

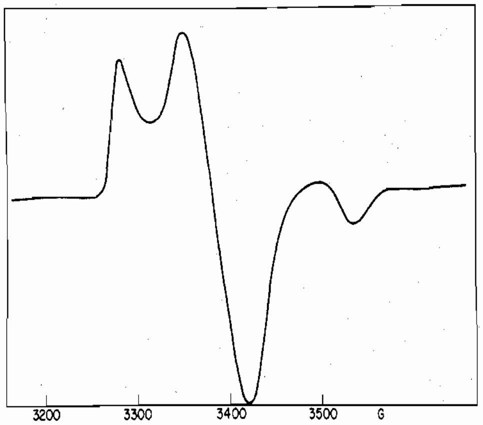

Figure 7. EPR spectrum of a frozen solution of $[Mo_2O(S_2CNEt_2)_2(C_6H_5CON_2)_2]^-$ in CH_2Cl_2 at 9.018 GHz and ~77 K.

with spectra previously observed for Mo(V) complexes in distorted trigonal-prismatic geometries[55-57]—these species are not particularly relevant models for the highly distorted environments of the dimers. Any conclusions based on comparisons of these purely qualitative observations are risky at best. The monomeric complex $Mo(S_2CNEt_2)(HNSC_6H_4)_2$,[58] which should be a closer structural analogue to the distorted trigonal-prismatic environment in the dimer, displays frozen glass spectra with a rhombic **g** tensor. Since the square-pyramidal Mo(III) species $(MoO(S_2CSC_3H_7)_2]^{-}$[38] also exhibits a three-line spectrum, the EPR results are equally consistent with the unpaired spin associated with the highly unsymmetric Mo_2N_2 dimer-bridge system or with a reduction resulting in the population of an orbital primarily localized on either Mo1 or Mo2. Although the effect on the potential of the reversible cathodic process of substitution of S for O in the diazenido ligand suggests that the electron transfer involves an orbital primarily localized on Mo1 and the X-ray crystallographic structure determination indicates that the Mo1 site is consistent with a d^0 configuration, the EPR studies fail to provide conclusive support that the redox process involves a localized Mo1 site.

In the absence of a more definitive investigation of the electronic properties of the dimers and of a detailed molecular orbital treatment of the bonding, discussions of the nature of the metal–metal interaction, and hence the description of the orbital involved in the reversible redox process, remain speculative.

Spectroscopic Studies. All the complexes have an intense IR band at about 950 cm^{-1} assigned to ν(Mo═O) for the terminal oxo group. The ^1H NMR spectra of some of the complexes are summarized in the Table II. For complex **4d**, the methylene protons of the dithiocarbamate ethyl groups appear as three quartets, the larger integrating as 4 protons and two smaller as 2 protons each. Inspection of the crystal structures (Figures 1 and 2) shows that the alkyl groups of the dithiocarbamate attached to Mo1 are inequivalent and the two quartets at 3.44 and 3.69 ppm are assigned to the ethyl groups of this ligand. The single quartet at 3.96 ppm is then assigned to the Mo2 dithiocarbamate methylene protons. The protons of the phenyl groups of the diazenido ligands appear as well-separated multiplets, the one to lower field being assigned to the ortho protons and the one to higher field to meta and para protons.

Acknowledgment. The structural and electrochemical investigations were supported by a grant (No. GM 22566) from the National Institutes of Health to J.Z.

Registry No. **4** (unsolvated), 67238-55-5; **3**, 67271-73-2; **4** (solvated), 67238-56-6; **4a**, 67238-57-7; **4b**, 67238-58-8; **4c**, 67238-59-9; **4d**, 67238-60-2; **4e**, 67238-61-3; $[MoO_2(S_2CNMe_2)_2]$, 18078-68-7; $[MoO_2(S_2CNEt_2)_2]$, 18078-69-8; $[MoO_2(S_2CN(CH_2)_5)_2]$, 21881-93-6; $PhCONHNH_2 \cdot HCl$, 1452-58-0; $PhCSNHNH_2$, 20605-40-7; *p*-$MeOC_6H_4CSNHNH_2$, 62625-55-2; *p*-$ClC_6H_4CSNHNH_2$, 50487-61-1; $[Mo_2O(S_2CNEt_2)_2(PhCON_2)_2]^-$, 67408-41-7; $[Mo_2O(S_2CNEt_2)_2(PhCSN_2)_2]^-$, 67408-40-6.

Supplementary Material Available: Listings of structure factor amplitudes (40 pages). Ordering information is given on any current masthead page.

References and Notes

(1) (a) University of Sussex. (b) State University of New York at Albany. (c) New York State Department of Health.
(2) J. T. Spence, *Coord. Chem. Rev.*, **4**, 475 (1969).
(3) (a) D. L. Stevenson and L. F. Dahl, *J. Am. Chem. Soc.*, **89**, 3721 (1967); (b) L. F. Dahl, D. Frisch, and G. Gust, Proceedings of the Climax First International Conference on the Chemistry and Uses of Molybdenum, University of Reading, P. C. H. Mitchell, Ed., Climax Molybdenum Co., London, 1973, p 134.
(4) (a) R. C. Burns and R. W. F. Hardy, *Methods Enzymol.*, **24**, 480 (1972); (b) W. A. Buelen and J. R. Le Comte, *ibid.*, **24**, 456 (1972); (c) V. K. Shek and W. J. Brill, *Biochim. Biophys. Acta*, **305**, 445 (1972).
(5) T. C. Huang, W. G. Zumft, and L. E. Mortenson, *J. Bacteriol.*, **113**, 884 (1973).
(6) (a) R. R. Eady, B. E. Smith, K. A. Cook, and J. R. Postgate, *Biochem. J.*, **128**, 655 (1972); (b) R. R. Eady, B. E. Smith, R. N. F. Thorneley, D. Ware, and J. R. Postgate, *Biochem. Soc. Trans.*, **1**, 37 (1973); (c) J. R. Postgate, personal communication, 1975.
(7) (a) R. C. Bray, P. C. Knowles, and L. S. Meriwether, *Wenner-Gren Cent. Int. Symp. Ser.*, **9**, 221 (1967); (b) R. C. Bray and J. C. Swann, *Struct. Bonding (Berlin)*, **11**, 207 (1972).
(8) W. E. Newton, J. L. Corbin, D. C. Bravard, J. E. Searles, and J. W. McDonald, *Inorg. Chem.*, **13**, 1100 (1974).
(9) G. J.-J. Chen, J. W. McDonald, and W. E. Newton, *Inorg. Chem.*, **15**, 2612 (1976).
(10) W. E. Newton, G. J.-J. Chen, and J. W. McDonald, *J. Am. Chem. Soc.*, **98**, 5388 (1976).
(11) L. J. DeHayes, H. C. Faulkner, W. M. Doub, Jr., and D. T. Sawyer, *Inorg. Chem.*, **14**, 2110 (1975).
(12) L. Ricard, J. Estienne, P. Karagiannidis, P. Toledano, J. Fischer, A. Mitschler and R. Weiss, *J. Coord. Chem.*, **3**, 277 (1974).
(13) A. B. Blake, F. A. Cotton, and J. S. Wood, *J. Am. Chem. Soc.*, **86**, 3024 (1964).
(14) J. R. Knox and C. K. Prout, *Acta Crystallogr., Sect. B*, **25**, 228 (1969).
(15) G. B. Maniloff and J. Zubieta, *Inorg. Nucl. Chem. Lett.*, **12**, 121 (1976).
(16) J. R. Knox and C. K. Prout, *Acta Crystallogr., Sect. B*, **25**, 1857 (1969).

(17) M. G. B. Drew and A. Kay, *J. Chem. Soc. A*, 1846 (1971).
(18) L. Ricard, C. Martin, R. West, and R. Weiss, *Inorg. Chem.*, **14**, 2300 (1975).
(19) B. Spivack, Z. Dori, and E. I. Stiefel, *Inorg. Nucl. Chem. Lett.*, **11**, 501 (1975).
(20) M. G. B. Drew and A. Kay, *J. Chem. Soc. A*, 1851 (1971).
(21) D. H. Brown and J. A. D. Jeffreys, *J. Chem. Soc., Dalton Trans.*, 732 (1973).
(22) L. Ricard, J. Estienne, and R. Weiss, *Inorg. Chem.*, **12**, 2182 (1973).
(23) J. I. Gelder and J. H. Enemark, *Inorg. Chem.*, **15**, 1839 (1976).
(24) B. Spivack and Z. Dori, *Coord. Chem. Rev.*, **17**, 99 (1975), and references therein.
(25) F. A. Cotton and S. M. Morehouse, *Inorg. Chem.*, **4**, 1377 (1965).
(26) G. T. J. Delbaere and C. K. Prout, *Chem. Commun.*, 162 (1971).
(27) B. Spivack, A. P. Gaughan, and Z. Dori, *J. Am. Chem. Soc.*, **93**, 5265 (1971).
(28) B. Spivack and Z. Dori, *J. Chem. Soc., Dalton Trans.*, 1173 (1973).
(29) (a) J. Chatt and J. R. Dilworth, *J. Less-Common Met.*, **86**, 531 (1974); (b) M. W. Bishop, J. Chatt, and J. R. Dilworth, *J. Organomet. Chem.*, **73**, C59 (1974); (c) M. W. Bishop, J. Chatt, J. R. Dilworth, G. Kaufman, S. Kim, and J. A. Zubieta, *J. Chem. Soc., Chem. Commun.*, 70 (1977).
(30) D. T. Cromer and J. T. Waber, *Acta Crystallogr.*, **18**, 104 (1965).
(31) R. F. Stewart, E. R. Davidson, and W. T. Simpson, *J. Chem. Phys.*, **42**, 3175 (1965).
(32) J. M. Stewart, G. J. Kruger, H. L. Ammon, C. Dickinson, and S. R. Hall, Technical Report TR-192, University of Maryland, June 1972.
(33) The same procedure has been followed by other authors, e.g., E. Sinn, *Inorg. Chem.*, **15**, 2698 (1976).
(34) M. J. Bennett, M. Cowie, J. L. Martin, and J. Takats, *J. Am. Chem. Soc.*, **95**, 7504 (1973).
(35) A. E. Smith, G. N. Schrauzer, V. P. Mayweg, and W. Heinrich, *J. Am. Chem. Soc.*, **87**, 5798 (1965).
(36) G. F. Brown and E. I. Stiefel, *Chem. Commun.*, 728 (1970).
(37) R. Hoffmann, J. M. Howell, and A. R. Rossi, *J. Am. Chem. Soc.*, **98**, 2484 (1976).
(38) J. Hyde, K. Venkatasubramanian, and J. Zubieta, *Inorg. Chem.*, **17**, 414 (1978).
(39) R. H. Summerville and R. Hoffmann, *J. Am. Chem. Soc.*, **98**, 7240 (1976).
(40) (a) J. Chatt, L. A. Duncanson, and L. M. Venanzi, *Nature (London)*, **177**, 1042 (1956); (b) R. Eisenberg, *Prog. Inorg. Chem.*, **12**, 295 (1970).
(41) S. Merlino, *Acta Crystallogr., Sect. B*, **24**, 1441 (1968).
(42) T. Brennan and I. Bernal, *J. Phys. Chem.*, **73**, 443 (1969).
(43) L. Pauling, "The Nature of the Chemical Bond", 3rd ed, Cornell University Press, Ithaca, N.Y., 1960.
(44) O. Bastiansen and A. De Meijera, *Angew. Chem.*, **78**, 142 (1966).
(45) J. Potenza and D. Mastropaolo, *Acta Crystallogr., Sect. B*, **29**, 1830 (1973).
(46) J. Potenza, R. J. Johnson, and D. Mastropaolo, *Acta Crystallogr., Sect. B*, **32**, 941 (1976).
(47) C. S. Harreld and E. O. Schlemper, *Acta Crystallogr., Sect. B*, **27**, 1964 (1971).
(48) A. Bondi, *J. Phys. Chem.*, **68**, 441 (1964).
(49) J. G. M. van de Aalsvoort and P. T. Beurskens, *Cryst. Struct. Commun.*, **3**, 653 (1974).
(50) E. L. Muetterties and L. J. Guggenberger, *J. Am. Chem. Soc.*, **96**, 1748 (1974).
(51) F. W. Moore and M. L. Larson, *Inorg. Chem.*, **6**, 998 (1967).
(52) W. Autenrieth and G. Thomas, *Chem. Ber.*, **57**, 423 (1923).
(53) K. A. Jensen and C. Pedersen, *Acta Chem. Scand.*, **15**, 1087 (1961).
(54) M. W. Bishop, J. Chatt, J. R. Dilworth, P. Vella, and J. Zubieta, manuscript in preparation.
(55) J. H. Waters, R. Williams, H. B. Gray, G. N. Schrauzer, and H. W. Finck, *J. Am. Chem. Soc.*, **86**, 4198 (1964).
(56) A. Davison, N. Edelstein, R. H. Holm, and A. H. Maki, *J. Am. Chem. Soc.*, **86**, 2799 (1964).
(57) E. I. Stiefel, *Prog. Inorg. Chem.*, **22**, 1 (1977).
(58) N. Pariyadath, W. E. Newton, and E. I. Stiefel, *J. Am. Chem. Soc.*, **98**, 5388 (1976).
(59) M. W. Bishop, J. Chatt, J. R. Dilworth, M. B. Hursthouse, and M. Motevalli, *J. Chem. Soc., Chem. Commun.*, 780 (1976).
(60) G. Bunzey, J. H. Enemark, J. K. Howie, and D. T. Sawyer, *J. Am. Chem. Soc.*, **99**, 4168 (1977).
(61) E. I. Stiefel, W. E. Newton, and N. Pariyadath, *J. Less-Common Met.*, **54**, 513 (1977).

Contribution from the Department of Chemistry,
The University of Michigan, Ann Arbor, Michigan 48109

Crystal and Molecular Structure of Bis(triphenylphosphine)rhodium(I) Chloride Dimer–Ethyl Acetate

M. DAVID CURTIS,* WILLIAM M. BUTLER, and JOHN GREENE

Received March 17, 1978

The structure of bis(triphenylphosphine)rhodium(I) chloride dimer has been determined by single-crystal X-ray diffraction techniques. The triclinic crystal ($a = 9.767$ (3), $b = 12.635$ (5), $c = 13.680$ (4) Å; $\alpha = 86.15$ (3), $\beta = 95.80$ (3), $\gamma = 100.84$ (3)°; $V = 1648$ Å^3), grown from ethyl acetate/methylene chloride solution, contained one molecule of rhodium dimer and one disordered molecule of ethyl acetate per unit cell. Intensity data were collected out to $2\theta = 45°$ with Mo Kα radiation. Of the 4964 reflections observed, 3007 had $I > 3\sigma(I)$ and were used in the full-matrix refinement. Assuming the space group $P\bar{1}$ (C_i^1, No. 2), the refinement converged at $R_1 = 0.045$ and $R_2 = 0.059$ with the rhodium dimer centered around the origin and the ethyl acetate of solvation disordered around the inversion center at 0, $^1/_2$, $^1/_2$. Some final structural parameters are Rh–Cl = 2.394 (2) and 2.424 (2) Å, Rh–P = 2.200 (2) and 2.213 (2) Å, Rh⋯Rh = 3.662 (2) Å, P–Rh–P = 96.34 (9)°, Rh–Cl–Rh = 98.95 (8)°, and Cl–Rh–Cl = 81.05 (8)°. The $RhCl_2Rh$ ring is planar, in contrast to all but one other of the rhodium(I) chloride dimers whose structures have been determined.

Dahl et al.[1] first reported the structure of a rhodium(I) chloride dimer $(CO)_2RhCl_2Rh(CO)_2$ and found the complex to be folded along the Cl⋯Cl axis. This folding has the effect of decreasing the Rh⋯Rh distance. To explain the observed folding, Dahl et al. proposed the existence of a bent Rh⋯Rh bond in the dimeric complex. Shortly thereafter, Ibers and Snyder[2] reported the structure of (COD)$RhCl_2Rh$(COD), which was found to be not folded as intuitively expected for two halide-bridged, four-coordinate d^8 centers. Since then, the structures of several other complexes of the general formula $L_2RhCl_2RhL_2$ have been solved and without exception the complexes have been folded along the Cl⋯Cl axis.[3-6]

The formation of a Rh–Rh bond in rhodium(I) chloride dimers has also received theoretical consideration. Summerville and Hoffmann[7] have applied the extended Hückel model to these complexes, focusing their attention on the molecular orbitals composed primarily of metal d orbitals. These authors found no primary interaction which would favor a folded structure over a planar one. In particular, the bonding effect from the overlap of d_{z^2} orbitals in the folded structure was cancelled by the corresponding antibonding MO which is also populated. Summerville and Hoffmann concluded that the folding distortion would be "soft" and that packing forces were most likely responsible for the observed distortions from planarity.

Norman and Gmur,[8] however, found a Rh–Rh bonding interaction in a low-lying MO which is primarily centered on the chloride ligands. The corresponding metal–ligand antibonding MO is not populated so that the net Rh–Rh bond order is greater in the folded structure than in the planar one.

0020-1669/78/1317-2928$01.00/0